Inorg. Chem. **2004**, *43*, 5891–5901

Solvation of Uranyl(II) and Europium(III) Cations and Their Chloro Complexes in a Room-Temperature Ionic Liquid. A Theoretical Study of the Effect of Solvent "Humidity"

Alain Chaumont and Georges Wipff*

Laboratoire MSM, UMR CNRS 7551, Institut de Chimie, 4 rue Blaise Pascal, 67 000 Strasbourg, France

Received May 11, 2004

We report a molecular dynamics study of the solvation of the UO_2^{2+} and Eu^{3+} cations and their chloro complexes in the [BMI][PF_6][H_2O] "humid" room-temperature ionic liquid (IL) composed of 1-butyl-3-methylimidazolium(+) and PF_6^- ions and H_2O in a 1:1:1 ratio. When compared to the results obtained in dry [BMI][PF_6], the present results reveal the importance of water. The "naked" cations form $UO_2(H_2O)_5^{2+}$ and $Eu(H_2O)_9^{3+}$ complexes, embedded in a shell of 7 and 8 PF_6^- anions, respectively. All studied $UO_2Cl_n^{2-n}$ and $EuCl_n^{3-n}$ chloro complexes remain stable during the dynamics and coordinate additional H_2O molecules in their first shell. $UO_2Cl_4^{2-}$ and $EuCl_6^{3-}$ are surrounded by an "unsaturated" water shell, followed by a shell of BMI^+ cations. According to an energy component analysis, the $UO_2Cl_4^{2-}$ and $EuCl_6^{3-}$ species, intrinsically unstable toward dissociation, are more stable than their less halogenated analogues in the IL solution, due to the solvation forces. The different chloro species also interact better with the humid than with the dry IL, which hints at the importance of solvent humidity to improve their solubility. Humidity markedly modifies the local ion environment, with major consequences as far as their spectroscopic properties are concerned. We finally compare the aqueous interface of [BMI][PF_6] and [OMI][PF_6] ionic liquids, demonstrating the importance of imidazolium substituents (*N*-butyl versus *N*-octyl) to the nature of the interface and miscibility with water.

Introduction

There is growing interest in room-temperature ionic liquids (hereafter denoted "ILs") as "green" (thermally and chemically stable, nonflammable, nonvolatile) solvents for metallic cations, especially in the context of nuclear waste partitioning.[1−5] ILs are based on organic cations (e.g., imidazolium, pyridinium, or ammonium derivatives) and anions whose choice allows the physicochemical properties, such as the miscibility with water, to be monitored and fine-tuned. With hydrophobic anions such as PF_6^- or $(CF_3SO_2)_2N^-$, imidazolium-based ILs form distinct phases with water, and can thus be used for liquid−liquid extraction purposes, yielding specific properties. Large distribution coefficients of metallic cations have been observed for ILs containing complexing agents. For instance, the Sr^{2+} extraction by dicyclohexano-18-crown-6 to ILs is several orders of magnitude larger than that to classical organic solvents.[4] Similar enhancements are observed for trivalent lanthanide or uranyl cations by phosphoryl-containing ligands (CMPO, TBP, CYANEX-type ligands), likely due to specific solvation features of the IL.[2] It is thus important to understand at the molecular level the solvation of the ions and their complexes in the IL solution. Important insights can be obtained by spectroscopies such as EXAFS,[6,7] UV−vis,[3] or luminescence.[8−10] A recent paper by Billard et al. hints at the

* Author to whom correspondence should be addressed. E-mail: wipff@chimie.u-strasbg.fr.

(1) Visser, A. E.; Swatloski, R. P.; Griffin, S. T.; Hartman, D. H.; Rogers, R. D. *Sep. Sci. Technol.* **2001**, *36*, 785−804.
(2) Visser, A. E.; Rogers, R. D. *J. Solid State Chem.* **2003**, *171*, 106−113.
(3) Dai, S.; Shin, Y. S.; Toth, L. M.; Barnes, C. E. *Inorg. Chem.* **1997**, *36*, 4900−4902.
(4) Dai, S.; Ju, Y. H.; Barnes, C. E. *J. Chem. Soc., Dalton Trans.* **1999**, 1201−1202.
(5) Barnes, C. E.; Shin, Y.; Saengkerdsub, S.; Dai, S. *Inorg. Chem.* **2000**, *39*, 862−864.
(6) Jensen, M. P.; Dzielawa, J. A.; Rickert, P.; Dietz, M. L. *J. Am. Chem. Soc.* **2002**, *124*, 10664−10665.
(7) Visser, A. E.; Jensen, M. P.; Laszak, I.; Nash, K. L.; Choppin, G.; Rogers, R. D. *Inorg. Chem.* **2003**, *42*, 2197−2199.
(8) Seddon, K. R.; Stark, A.; Torres, M. J. *Pure Appl. Chem.* **2000**, *72*, 2275−2287.

10.1021/ic049386v CCC: $27.50
Published on Web 08/27/2004

complexity and versatility of the Eu^{III} ion environment as a function of the IL humidity and of the amount of Cl^- anions in the solution.[11] Computer simulations also contribute to our understanding of the solvent structure and solvation properties. Quantum mechanical methods allow the fundamental interactions between selected components of the system to be "accurately" described,[12−17] but are not sufficient to depict the dynamics and complexity of solutions. Insights into those features can be obtained by molecular dynamics (MD) or Monte Carlo methods, based on empirical representations of the potential energy.[18−27] This led us to investigate the solvation of lanthanide M^{3+} and uranyl cations in ILs that are based on 1-alkyl-3-methylimidazolium(+) and PF_6^- or $AlCl_4^-$ anions. The first studies dealt with "ideal" ILs,[28−30] while the effect of liquid (Lewis) "basicity" was also investigated,[31] allowing us to depict the interactions among $Eu^{III}Cl_n^{3-n}$, $Eu^{II}Cl_n^{2-n}$, and $UO_2Cl_n^{2-n}$ complexes and the liquid as a function of the number of Cl^- ligands.[31] These exploratory simulations were based on a "dry" IL model, without water. It is known from experiment, however, that imidazolium-based ILs used for liquid−liquid extraction purposes are hygroscopic. Their water content decreases with temperature and, for a given anion, when imidazolium substituents become more hydrophobic.[8,32−35] It is thus important to determine the role of water in the solvation properties of the IL.

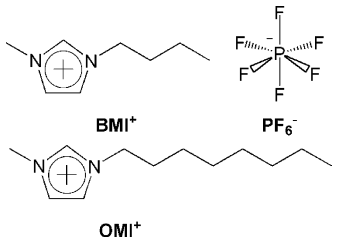

Figure 1. Components of the simulated humid IL.

In this Article, we report an MD study of the solvation of the Eu^{3+} and UO_2^{2+} "naked" cations and their chloro complexes in the [BMI][PF_6][H_2O] humid IL, based on BMI^+ (1-butyl-3-methylimidazolium) and PF_6^- ions (Figure 1). This model solution contains one H_2O molecule per $BMI^+PF_6^-$ ion pair. This is somewhat more than the experimental value of water solubility in the pure [BMI][PF_6] liquid (2.3% in weight, i.e., 0.26 in mole fraction),[32] but reasonably models the [BMI][PF_6] IL containing some amounts of hydrophilic species such as europium or uranyl cations or their chloro complexes, in equilibrium with uncomplexed Cl^- anions. Also note that the water solubility in the IL can double when the imidazolium *N*-butyl group is replaced by *N*-methyl.[33] Our main aims are to compare the ion solvation in the humid versus dry ILs from the structural and energetical points of view, and to gain insights into the relative stability of the different chloro complexes in solution. The question of water mixing with the IL will also be addressed from the point of view of the IL/water "interface", which presumably plays a key role in assisted ion extraction.

Methods

Molecular Dynamics. The systems were simulated by classical MD using the modified AMBER 7.0 software[36] in which the potential energy U is described by a sum of bond, angle, and dihedral deformation energies and pairwise additive 1−6−12 (electrostatic + van der Waals) interactions between nonbonded atoms:

$$U = \sum_{\text{bonds}} k_b(b - b_0)^2 + \sum_{\text{angles}} k_\theta(\theta - \theta_0)^2 + \sum_{\text{dihedrals}} \sum_n V_n(1 + \cos(n\varphi - \gamma) + \sum_{i<j}\left[\frac{q_i q_j}{R_{ij}} - 2\epsilon_{ij}\left(\frac{R_{ij}^*}{R_{ij}}\right) + \epsilon_{ij}\left(\frac{R_{ij}^*}{R_{ij}}\right)^{12}\right]$$

Cross-terms in van der Waals interactions were constructed using the Lorentz−Berthelot rules. The BMI^+ ion parameters are taken

(9) Mele, A.; Tran, C. D.; Lacerda, S. H. D. P. *Angew. Chem., Int. Ed.* **2003**, *42*, 4364−4366.
(10) Billard, I.; Moutiers, G.; Labet, A.; ElAzzi, A.; Gaillard, C.; Mariet, C.; Lutzenkirchen, K. *Inorg. Chem.* **2003**, *42*, 1726−1733.
(11) Billard, I.; Mekki, S.; Gaillard, C.; Hesemann, P.; Moutiers, G.; Mariet, C.; Labet, A.; Bünzli, J.-C. G. *Eur. J. Inorg. Chem.* **2004**, 1190−1197.
(12) Dymek, C. J. J.; Stewart, J. J. P. *Inorg. Chem.* **1989**, *28*, 1472.
(13) Takahashi, S.; Suzuya, K.; Kohara, S.; Koura, N.; Curtiss, L. A.; Saboungi, M. L. *Z. Phys. Chem. (Muenchen)* **1999**, *209*, 209−211.
(14) Sitze, M. S.; Schreiter, E. R.; Patterson, E. V.; Freeman, R. G. *Inorg. Chem.* **2001**, *40*, 2298−2304.
(15) Meng, Z.; Dolle, A.; Carper, W. R. *J. Mol. Struct.: THEOCHEM* **2002**, *585*, 119−128.
(16) Turner, E. A.; Pye, C. C.; Singer, R. D. *J. Phys. Chem. A* **2003**, *107*, 2277−2288.
(17) Li, X. Y.; Nie, J. *J. Phys. Chem. A* **2003**, *107*, 6007−6013.
(18) Shah, J. K.; F.Brennecke, J.; Maginn, E. J. *Green Chem.* **2002**, *4*, 112−118.
(19) Morrow, T. I.; Maginn, E. J. *J. Phys. Chem. B* **2002**, *106*, 12807−12813.
(20) Hanke, C. G.; Atamas, N. A.; Lynden-Bell, R. M. *Green Chem.* **2002**, *4*, 107−111.
(21) Hanke, C. G.; Price, S. L.; Lynden-Bell, R. M. *Mol. Phys.* **2001**, *99*, 801−809.
(22) de Andrade, J.; Böes, E. S.; Stassen, H. *J. Phys. Chem. B* **2002**, *106*, 13344−13351.
(23) Popolo, M. G. D.; Voth, G. A. *J. Phys. Chem. B* **2004**, *108*,
(24) Margulis, C. J.; Stern, H. A.; Berne, B. J. *J. Phys. Chem. B.* **2002**, *106*, 12017−12021.
(25) Lynden-Bell, R. M.; Atamas, N. A.; Vasilyuk, A.; Hanke, C. G. *Mol. Phys.* **2002**, *100*, 3225−3229.
(26) Znamenskiy, V.; Kobrak, M. N. *J. Phys. Chem. B* **2004**, *108*, 1072−1079.
(27) Jensen, M. P.; Neuenfeind, J.; Beitz, J. V.; Skanthakumar, S.; Sonderholm, L. *J. Am. Chem. Soc.* **2003**, *125*, 15466−15473 and references therein.
(28) Chaumont, A.; Engler, E.; Wipff, G. *Inorg. Chem.* **2003**, *42*, 5348−5356.
(29) Chaumont, A.; Wipff, G. *Phys. Chem. Chem. Phys.* **2003**, *5*, 3481−3488.
(30) Chaumont, A.; Wipff, G. *J. Phys. Chem. A* **2004**, *108*, 3311−3319.
(31) Chaumont, A.; Wipff, G. *Chem.−Eur. J.* **2004**, *10*, 3919−3930.
(32) Anthony, J. L.; Maginn, E. J.; Brennecke, J. F. *J. Phys. Chem. B* **2001**, *105*, 10942−10949.
(33) Wong, D. S. H.; Chen, J. P.; Chang, J. M.; Chou, C. H. *Fluid Phase Equilib.* **2002**, *194−197*, 1089−1095.
(34) Huddleston, J. G.; Visser, A. E.; Reichert, W. M.; Willauer, H. D.; Broker, G. A.; Rogers, R. D. *Green Chem.* **2001**, *3*, 156−164.
(35) Gutowski, K. E.; Broker, G. A.; Willauer, H. D.; Huddleston, J. G.; Swatloski, R. P.; Holbrey, J. D.; Rogers, R. D. *J. Am. Chem. Soc.* **2003**, *125*, 6632−6633.
(36) Case, D. A.; Pearlman, D. A.; Caldwell, J. W.; Cheatham, T. E., III; Wang, J.; Ross, W. S.; Simmerling, C. L.; Darden, T. A.; Merz, K. M.; Stanton, R. V.; Cheng, A. L.; Vincent, J. J.; Crowley, M.; Tsui, V.; Gohlke, H.; Radmer, R. J.; Duan, Y.; J. Pitera; Massova, I.; Seibel, G. L.; Singh, U. C.; Weiner, P. K.; Kollman, P. A. *AMBER7*; University of California: San Francisco, 2002.

from ref 22, while those of PF_6^- are from the OPLS force field[37] and have been tested on the pure liquid properties.[22,28] The van der Waals parameters for UO_2^{2+} ($R_U^* = 1.58$ Å; $\epsilon_U = 0.4$ kcal/mol)[38] and Eu^{3+} ($R_{Eu}^* = 1.852$ Å; $\epsilon_{Eu} = 0.05$ kcal/mol)[39] were fitted to free energies of hydration and also correctly account for the hydration numbers of these cations and for the corresponding cation−water coordination distances in aqueous solution. Despite the lack of explicit polarization and nonadditivity terms, these 1−6−12 potentials also account for the relative stabilities of the europium and uranyl chloro complexes in the gas phase, as compared to QM results (vide infra). Water is described by the TIP3P model.[40] The 1−4 van der Waals interactions were scaled down by a factor of 2.0, and the 1−4 Coulombic interactions were scaled down by 1.2. The solutions were simulated with 3D-periodic boundary conditions. Nonbonded interactions were calculated with a 12 Å atom based cutoff, correcting for the long-range electrostatics by using the Ewald summation method (PME (particle−particle mesh Ewald) approximation).[41]

The MD simulations were performed at 300 K starting with random velocities. The temperature was monitored by coupling the system to a thermal bath using the Berendsen algorithm[42] with a relaxation time of 0.2 ps. In the NPT simulations, the pressure was similarly coupled to a barostat with a relaxation time of 0.2 ps. All C−H bonds were constrained with SHAKE, using the Verlet leapfrog algorithm with a time step of 2 fs to integrate the equations of motion.

We first equilibrated "cubic" boxes of the pure liquid, by repeated sequences of (i) heating the system at 500 K at constant volume for 0.5 ns followed by (ii) 0.5 ns of dynamics at 300 K and a constant pressure of 1 atm and (iii) 1 ns of dynamics at 300 K and constant volume. The final box was simulated in the NVT ensemble for 2 ns at 300 K.

The uranyl or europium ions or their complexes were immersed in the ionic liquid while BMI^+ or PF_6^- solvent ions were removed to keep the box neutral. The solvent boxes with a single metal ion are cubic (∼43 Å in length) and contain ∼200 (BMI^+, PF_6^-, H_2O) molecules. More concentrated solutions of UO_2^{2+} and Eu^{3+} ions (with nine cations per box) were also simulated with larger boxes. Details are given in Table 1. Equilibration of the europium or uranyl solutions started with 1500 steps of steepest descent energy minimization, followed by 50 ps of MD at 300 K with fixed solutes ("BELLY" option of AMBER) at constant volume and by 50 ps without constraints, followed by 50 ps at a constant pressure of 1 atm. The subsequent MD trajectories were run from 2 ns and saved every 0.5 ps.

The MD simulations on the IL/water "mixtures" (i.e., at the preformed IL/water interface and for mixing/demixing simulations) started with adjacent boxes of IL and water of similar volumes. Their characteristics are given in Table S2 in the Supporting Information. After a sequence of energy minimization, 50 ps of MD at 300 K in the NVT ensemble, and 50 ps in the NPT ensemble ($P = 1$ atm), the dynamics was run for 10 ns at constant volume. The mixing of the two phases was obtained by subsequent dynamics of 1 ns at 600 K with biased potentials (Coulombic interactions scaled down by a factor of 100). The "demixing" dynamics was run at 300 K at constant volume with reset potentials for 10 ns.

Table 1. Characteristics of the Simulated Uranyl and Europium Ionic Liquid Solutions

system	BMI^+	PF_6^-	H_2O	box size (Å^3)	time (ns)
UO_2^{2+}	200	202	200	42.5	4.5
UO_2Cl_2	200	200	200	42.6	4.5
$UO_2Cl_3^-$	201	200	200	42.6	4.5
$UO_2Cl_4^{2-}$	202	200	200	42.6	4.5
9 UO_2^{2+}	432	450	450	55.4	2
Eu^{3+}	200	203	200	42.6	4.5
$EuCl_3$	200	200	200	42.5	4.5
$EuCl_4^-$	201	200	200	42.6	4.5
$EuCl_5^{2-}$	202	200	200	42.7	4.5
$EuCl_6^{3-}$	203	200	200	42.7	4.5
9 Eu^{3+}	423	450	450	55.1	5

The trajectories were analyzed with the MDS and DRAW software.[43] The average solvation structure was characterized by the radial distribution functions (RDFs) of the P_{PF_6}, O_{H_2O}, and *N*-butyl$_{BMI}$ atoms of the solvent around the U_{UO_2} or Eu atoms during the last 0.2 ns. Insights into the energy component were obtained by group analysis, using a 17 Å cutoff distance and a reaction field correction for the electrostatics.[44] Typical snapshots were redrawn with VMD.[45] The diffusion coefficients D were calculated from the Einstein equation (in principle valid for an "infinite" time): $6Dt = \langle [r_i(t) - r_i(0)]^2 \rangle$ over 2 ns.

Quantum Mechanical Calculations. The UO_2Cl_2, $UO_2Cl_3^-$, and $UO_2Cl_4^{2-}$ complexes were optimized at the Hartree−Fock (HF) and DFT (B3LYP functional) levels of theory, using the Gaussian98 software.[46] The Cl and O atoms were described by the 6-31+G* basis set. For uranium, we used a relativistic large-core effective core potential (ECP) of the Los Alamos group[47] with 78 electrons in the core and a [3s,3p,2d,2f] contracted valence basis set. The binding energies of the Cl^- ligands have been corrected for basis set superposition errors (BSSEs).[48] Total energies and optimized structures and their Mulliken charges are given in Table S1 in the Supporting Information. The $PF_6^-\cdots H_2O$ and $BMI^+\cdots OH_2$ dimers were similarly optimized by HF/6-31+G* and by DFT/6-31+G* calculations.

(37) Kaminski, G. A.; Jorgensen, W. L. *J. Chem. Soc., Perkin Trans. 2* **1999**, *2*, 2365−2375. It should be noted that the OPLS force field uses a different mixing rule, compared to AMBER (i.e., the geometric instead of the arithmetic mean for the van der Waals radii). Our results are, however, reasonable (see, e.g., the density of the liquid and the PF_6^-/H_2O interaction energies calculated by QM/AMBER (see ref 52)).

(38) Guilbaud, P.; Wipff, G. *J. Mol. Struct.: THEOCHEM* **1996**, *366*, 55−63.

(39) van Veggel, F. C. J. M.; Reinhoudt, D. *Chem.−Eur. J.* **1999**, *5*, 90−95.

(40) Jorgensen, W. L.; Chandrasekhar, J.; Madura, J. D.; Impey, R. W.; Klein, M. L. *J. Chem. Phys.* **1983**, *79*, 926−936.

(41) Darden, T. A.; York, D. M.; Pedersen, L. G. *J. Chem. Phys.* **1993**, *98*, 10089.

(42) Berendsen, H. J. C.; Postma, J. P. M.; van Gunsteren, W. F.; DiNola, A. *J. Chem. Phys.* **1984**, *81*, 3684−3690.

(43) Engler, E.; Wipff, G. In *Crystallography of Supramolecular Compounds*; Tsoucaris, G., Ed.; Kluwer: Dordrecht, The Netherlands, 1996; pp 471−476.

(44) Tironi, I. G.; Sperb, R.; Smith, P. E.; van Gunsteren, W. F. *J. Chem. Phys.* **1995**, *102*, 5451−5459.

(45) Humphrey, W.; Dalke, A.; Schulten, K. *J. Mol. Graphics* **1996**, *14*, 33−38.

(46) Frisch, M. J.; Trucks, G. W.; Schlegel, H. B.; Scuseria, G. E.; Robb, M. A.; Cheeseman, J. R.; Zakrzewski, V. G.; Montgomery, J. A., Jr.; Stratmann, R. E.; Burant, J. C.; Dapprich, S.; Millam, J. M.; Daniels, A. D.; Kudin, K. N.; Strain, M. C.; Farkas, O.; Tomasi, J.; Barone, V.; Cossi, M.; Cammi, R.; Mennucci, B.; Pomelli, C.; Adamo, C.; Clifford, S.; Ochterski, J.; Petersson, G. A.; Ayala, P. Y.; Cui, Q.; Morokuma, K.; Malick, D. K.; Rabuck, A. D.; Raghavachari, K.; Foresman, J. B.; Cioslowski, J.; Ortiz, J. V.; Stefanov, B. B.; Liu, G.; Liashenko, A.; Piskorz, P.; Komaromi, I.; Gomperts, R.; Martin, R. L.; Fox, D. J.; Keith, T.; Al-Laham, M. A.; Peng, C. Y.; Nanayakkara, A.; Gonzalez, C.; Challacombe, M.; Gill, P. M. W.; Johnson, B.; Chen, W.; Wong, M. W.; Andres, J. L.; Gonzalez, C.; Head-Gordon, M.; Replogle, E. S.; Pople, J. A. *Gaussian 98*, Revision A.5; Gaussian, Inc.: Pittsburgh, PA, 1998.

(47) Ortiz, J. V.; Hay, P. J.; Martin, R. L. *J. Am. Chem. Soc.* **1992**, *114*, 2736−2737 and references therein.

(48) Boys, S. F.; Bernardi, F. *Mol. Phys.* **1970**, *19*, 553−566.

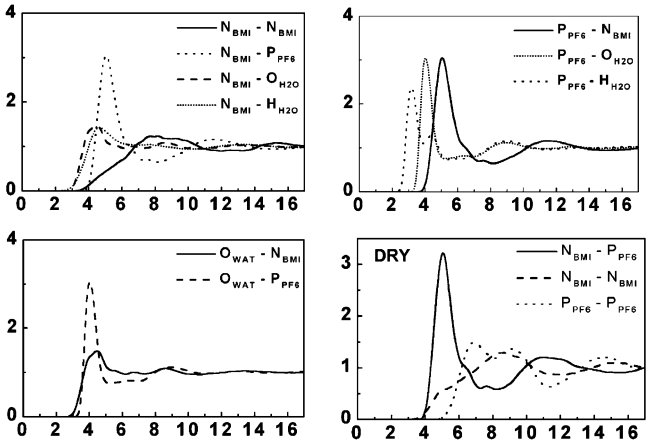

Figure 2. Neat [BMI][PF_6][H_2O] humid liquid: radial distribution functions as a function of the distances (Å) (averages over the last 0.2 ns). Typical snapshots are given in Figures 3 and S1.

Results

We first describe the main characteristics of the neat humid liquid (section 1), and next examine the solvation of the uranyl and europium cations and their chloro complexes. The simulations demonstrate the importance of the ionic liquid humidity to the solvation of the free europium and uranyl cations and their chloro complexes. During the dynamics, all chloro complexes remained bonded. The unsaturated $UO_2Cl_n^{2-n}$ (n = 0, 2, or 3) and $EuCl_n^{3-n}$ (n = 3−5) complexes completed their inner shell with H_2O molecules, while the saturated $UO_2Cl_4^{2-}$ and $EuCl_6^{3-}$ complexes became solvated by a first shell of water molecules. Details are given in sections 2 and 3, and energy features are analyzed in section 4. In the Discussion of this Article, we compare two neat binary IL/water systems, with BMI^+ versus OMI^+ cations (Figure 1).

1. Characteristics of the Neat Humid [BMI][PF_6][H_2O] Liquid. The calculated density of the humid liquid (1.30 kg dm^{-3}) is close to, but somewhat smaller than, the calculated and experimental densities of the dry liquid (1.32 kg dm^{-3} [28] and 1.36−1.37 kg dm^{-3},[49,50] respectively), which is consistent with the small excess volume of mixing calculated for analogous systems.[51]

The solvent diffusion is faster in the humid than in the dry IL, as indicated by the average diffusion coefficients D. The D values (10^6 cm^2 s^{-1}) in the humid versus dry solvents are 0.26 versus 0.04 for P_{PF_6} and 0.29 versus 0.04 for N_{BMI}. The water diffusion in the humid IL is still faster (5.2×10^{-6} cm^2 s^{-1}). This is why the sampling of the solvent configurations should be more efficient in the humid than in the dry liquid.

The average structure of the humid IL is characterized by the RDFs of N_{BMI}, P_{PF_6}, and O_{OH_2} (see Figure 2; their characteristics are summarized in Table 2). As in the dry IL, one sees loose cation−anion contacts, corresponding to a peak of 5.1 PF_6^- anions, on the average, around each BMI^+ cation, and vice versa. Water is "randomly" distributed in the box, and displays specific interactions with the liquid ions and with itself. A visual inspection of the trajectories at the graphic systems reveals that there is more water around the PF_6^- anions than the BMI^+ cations, which hints at stronger interactions with the former.[52] This is supported by an energy component analysis on the IL which shows that the interaction energy of one H_2O molecule with the IL components follows the order PF_6^- (−7.7 kcal/mol) > BMI^+ (−3.0 kcal/mol) > H_2O (−2.2 kcal/mol), on the average. Some H_2O molecules are hydrogen bonded to the C_2H and C_4H, C_5H imidazolium protons (0.6 H_2O molecule, on the average per proton, at 2.5 and 2.7 Å, respectively). Water also acts as a proton donor to the PF_6^- anion (∼1.5 H_{wat} and 1.5 O_{wat} atoms, on the average), as seen from the P···H_{wat} and P···O_{wat} peaks in the RDFs (3.2 and 4.0 Å, respectively). This is indicative of dominant "linear" hydrogen bonds, but H_2O molecules sometimes bridge over two F atoms of the anion, as found in the optimized PF_6···H_2O dimer.[53] One also finds O_{wat}···H_{wat} hydrogen bonds (1.3, on the average, at 2.8 Å), corresponding to small water oligomers, in equilibrium with H_2O monomers (Figure S1 in the Supporting Information). There are also some aggregates of 6−10 H_2O molecules, reminiscent of clathrate-type arrangements around PF_6^- anions. Water sometimes acts as a "glue" between ionic components, e.g., via bridging PF_6^-···HOH··· PF_6^- interactions, or CH_{BMI}···OH_2···PF_6^- interactions (see Figure 3).

Table 2. Neat Humid [BMI][PF_6][H_2O]: Characteristics of the First Peak of the Radial Distribution Functions[a]

N_{BMI}−N_{BMI}	18.2 (7.9, 12.0)	P_{PF_6}−N_{BMI}	5.1 (5.1, 7.3)
N_{BMI}−P_{PF_6}	5.0 (5.1, 7.3)	P_{PF_6}−O_{H_2O}	1.8 (4.0, 5.3)
N_{BMI}−O_{H_2O}	2.5 (4.5, 6.2)	P_{PF_6}−H_{H_2O}	1.5 (3.2, 3.9)
N_{BMI}−H_{H_2O}	7.5 (4.7, 7.0)	O_{H_2O}−N_{BMI}	1.8 (4.0, 5.3)
$H5_{BMI}$−O_{H_2O}	0.6 (2.5, 3.8)	O_{H_2O}−P_{PF_6}	2.5 (4.5, 6.2)
$H4_{BMI}$−O_{H_2O}	0.6 (2.7, 4.0)	O_{H_2O}−O_{H_2O}	1.3 (2.8, 3.7)

[a] Coordination number (first line) and positions (Å) of the first maximum and minimum (second line). Averages over the last 0.2 ns.

2. Uranyl Cation and Its Chloro Complexes in the Humid [BMI][PF_6][H_2O] Liquid. The naked UO_2^{2+} cation

(49) Gu, Z.; Brennecke, J. F. *J. Chem. Eng. Data* **2002**, *47*, 339.
(50) Suarez, P. A. Z.; Einloft, S.; Dullius, J. E. L.; de Souza, R. F.; Dupont, J. *J. Chim. Phys. Phys.-Chim. Biol.* **1998**, *95*, 1626.
(51) Hanke, C. G.; Lynden-Bell, R. M. *J. Phys. Chem. B* **2003**, *107*, 10873−10878.

(52) According to AMBER force field and BSSE corrected QM calculations on the optimized PF_6^-···H_2O and BMI^+···OH_2 dimers (hydrogen bonded to water via the C_2H proton), the water binding energies to PF_6^- and to BMI^+ are however similar (9.1 and 9.7 kcal/mol at the HF level, 9.5 and 9.5 kcal/mol at the DFT level, and 10.4 and 9.2 kcal/mol with the AMBER force field). This suggests that the favored hydration of PF_6^-, compared to BMI^+, in the ionic liquid results from entropy effects, due to the larger accessible surface of PF_6^-, compared to the restricted binding C_2H region of BMI^+ or MMI^+ ions. Also notice the good agreement between the QM and AMBER interaction energies. Surprisingly, the experimental enthalpy of water absorption by the [BMI][PF_6] ionic liquid (7.2 kcal/mol)[32] is smaller than the individual PF_6^-···H_2O or BMI^+···OH_2 interaction energies.
(53) According to the AMBER calculations, the (bridging) hydrogen bond energy of H_2O with PF_6^- amounts to 10.4 kcal/mol, which is in good agreement with the QM-calculated values (including BSSE corrections) of 9.1 kcal/mol (HF/6-31+G* calculation) and 9.1 kcal/mol (DFT-B3LYP/6-31+G* calculation).

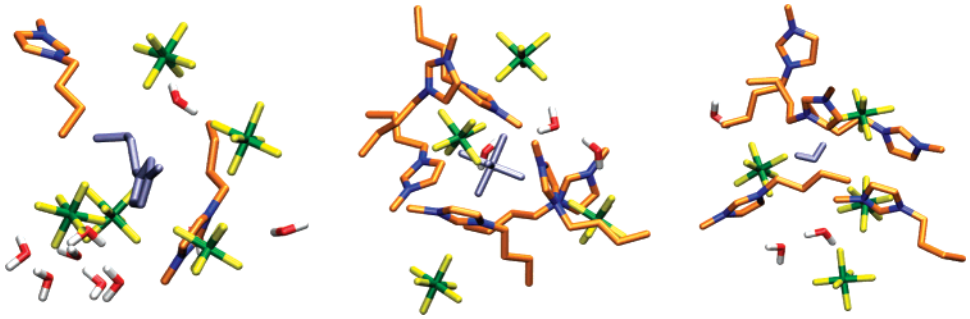

Figure 3. Neat [BMI][PF_6][H_2O] humid liquid. Typical snapshots of ions in interaction and water.

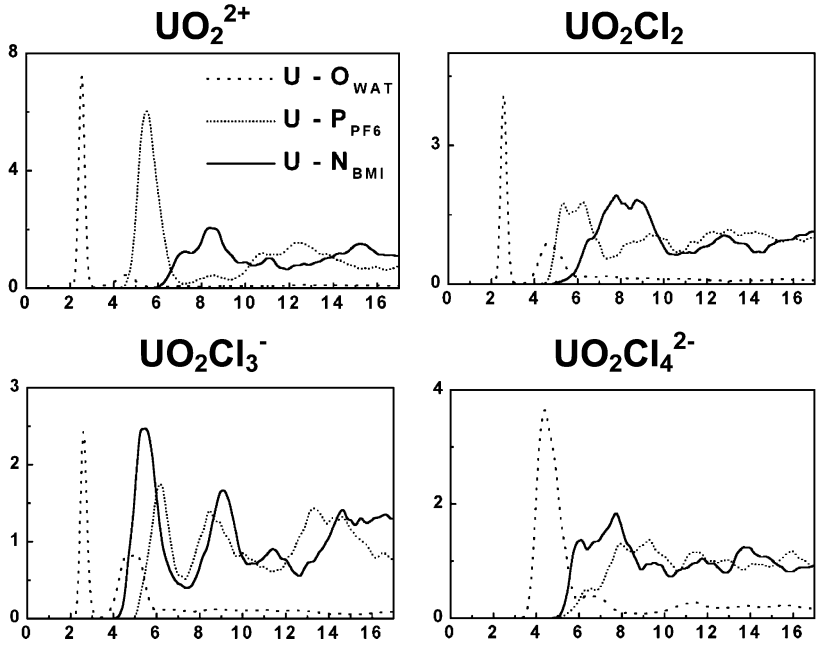

Figure 4. UO_2^{2+} and its chloro complexes in the humid IL solution: RDFs of O_{wat}, P_{PF_6}, and N_{BMI} atoms around the U atom.

captured in less than 0.5 ns water molecules to form the pentahydrated $UO_2(H_2O)_5^{2+}$ complex, as in pure water.[54,55] Nine such complexes also formed in less than 0.5 ns in the more concentrated uranyl solution. From the time evolution of the uranyl hydration numbers (Figure S2 in the Supporting Information), it can be seen that 6 of the 9 uranyl cations are hydrated in less than 0.1 ns, and that the other 3 gradually evolve from tri- to pentacoordination in 0.3−1.1 ns. The RDFs and typical snapshots are shown in Figures 4 and 5. The RDF characteristics are summarized in Table 3. In the second shell of $UO_2(H_2O)_5^{2+}$, one finds 6.9 PF_6^- anions, on the average, within 7.2 Å. This anionic shell is not "saturated", but penetrated by water molecules (about 5 H_2O molecules on the average), which form "water fingers" with about two of the equatorial H_2O molecules (Figure S1). The other three equatorial H_2O molecules are locked between uranyl and PF_6^- anions. Beyond the PF_6^- shell, one finds 11.7 BMI^+ cations on the average, within 10.4 Å, and water molecules.

The unsaturated UO_2Cl_2 and $UO_2Cl_3^-$ complexes similarly captured 3.0 and 2.0 H_2O molecules, respectively, thus achieving equatorial coordination numbers of 5, but display more complex second shell arrangements. The $UO_2Cl_2(H_2O)_3$ complex, although neutral, further binds ∼4.0 PF_6^- anions (within 7.4 Å), ∼14 BMI^+ cations (within 10.6 Å), and an important water network (12 H_2O molecules within 7.4 Å). The negatively charged $UO_2Cl_3^-(H_2O)_2^-$ complex is similarly surrounded by water (11 H_2O molecules) and a mixture of "loosely bound" 2.7 PF_6^- anions and 3.9 BMI^+ cations.

The saturated $UO_2Cl_4^{2-}$ complex is hydrogen bonded to a first shell of 12.5 water molecules, on the average, embedded inside a disordered cage of 8.0 BMI^+ cations (within 8.9 Å). About two H_2O molecules display bridging interactions over two chloride ligands, while the others are "monodentate".

3. Europium(III) Cation and Its Chloro Complexes in the Humid Liquid. The solvation of the Eu^{3+} cation and its chloro complexes displays marked analogies with the solvation of uranyl. The RDFs and typical snapshots are shown in Figures 6 and 7. A snapshot of water alone is given in Figure S1. First, in the absence of chloro ligands, Eu^{3+} forms a fully hydrated $Eu(H_2O)_9^{3+}$ complex, as in pure water and in the solid state structures with poorly coordinating anions such as $CF_3SO_3^-$.[56,57] This complex is observed in

(54) Neuefeind, J.; Soderholm, L.; Skanthakumar, S. *J. Phys. Chem. A* **2004**, *108*, 2733−2739.
(55) Guilbaud, P.; Wipff, G. *J. Phys. Chem.* **1993**, *97*, 5685−5692 and references cites therein.

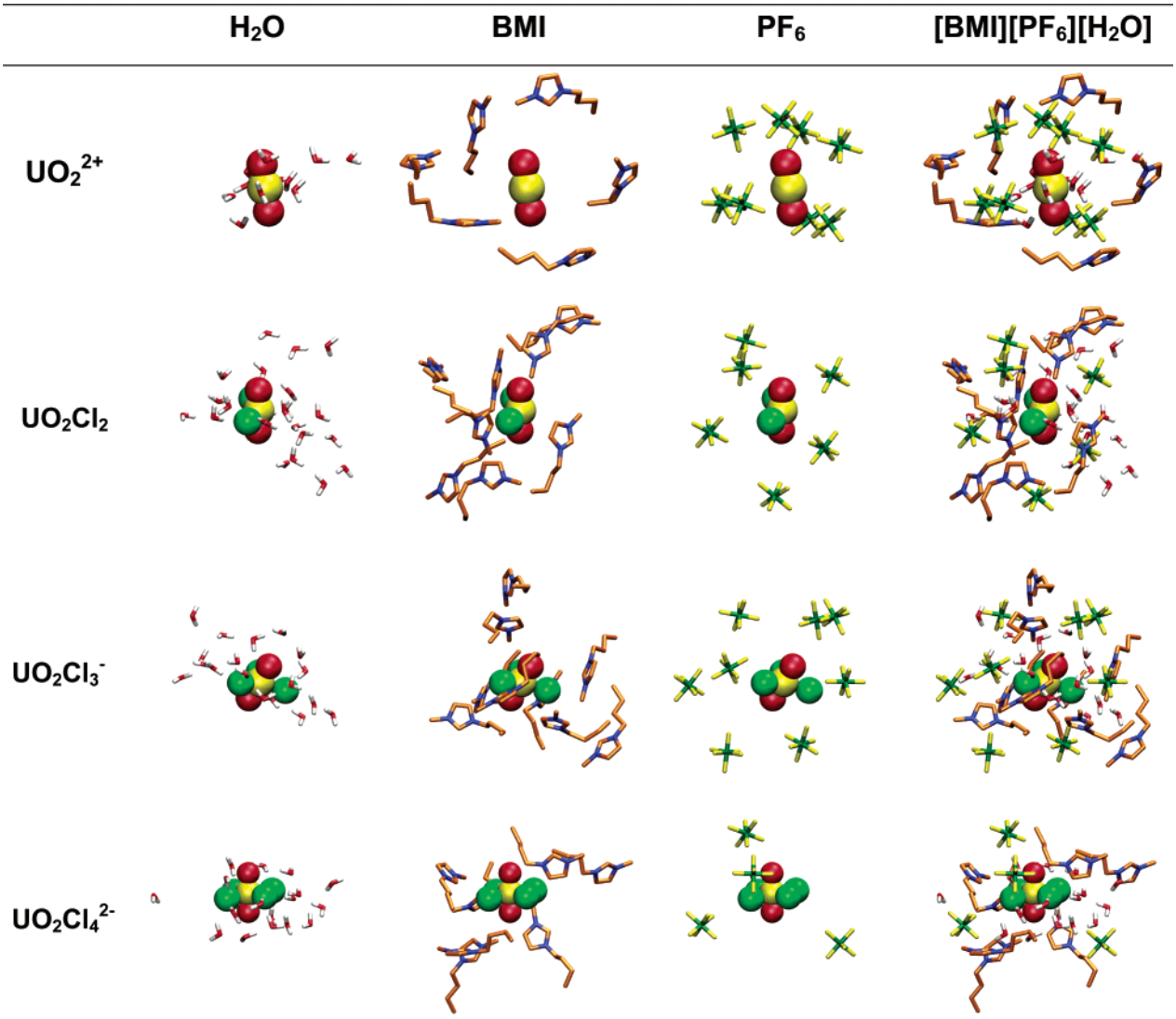

Figure 5. UO_2^{2+} and its chloro complexes in the humid IL solution: final snapshots of the first shell (within 9 Å) of U, showing (from left to right) H_2O only, BMI^+ only, PF_6^- only, and the solvent.

the simulations of the "diluted" solution, and for 7 of the 9 Eu^{3+} cations in the more concentrated solution (Figure S3). In the latter case, however, one Eu^{3+} cation remained trihydrated only, and another one was not hydrated at all after 5 ns. The reason can be found in the too low local concentration of water in some cases, and in the reduced "free water" content, once an important amount has been complexed by the other Eu^{3+} cations. The most abundant $Eu(H_2O)_9^{3+}$ complex is surrounded by a shell of 8.0 PF_6^- anions (within 7.0 Å), followed by 13.0 BMI^+ cations (within 10.4 Å).

The unsaturated $EuCl_3$, $EuCl_4^-$, and $EuCl_5^{2-}$ complexes bind 5.0, 3.0, and 2.0 inner shell H_2O molecules, respectively, leading to europium coordination numbers of 8, 7, and 7. Despite the lack of electrostatic attractions with the former complex or the repulsions with the two latter ones, these are next surrounded by PF_6^- anions (5.0, 2.7, and 2.0,

Table 3. UO_2^{2+} and Eu^{3+} Cations and Their Chloride Complexes in Humid Solution: Characteristics of the First Peak of the Radial Distribution Functions around the U and Eu Atoms[a]

system	O_{wat}	P_{PF_6}	N_{BMI}
UO_2^{2+}	5.0 (0.1)	6.9 (0.3)	11.7 (1.1)
	(2.6, 3.1)	(5.5, 7.2)	(8.4, 10.4)
UO_2Cl_2	3.0 (0.1)	4.0 (0.6)	13.6 (1.2)
	(2.6, 3.2)	(5.4, 7.4)	(7.8, 10.6)
$UO_2Cl_3^-$	2.0 (0.0)	2.7 (0.7)	3.9 (0.4)
	(2.6, 3.4)	(6.2, 7.3)	(5.5, 7.4)
$UO_2Cl_4^{2-}$	12.5 (1.7)	11.3 (1.0)	8.0 (1.0)
	(4.4, 6.0)	(8.0, 10.7)	(7.7, 8.9)
Eu^{3+}	9.0 (0.0)	8.0 (0.2)	13.0 (0.8)
	(2.5, 3.3)	(5.6, 7.0)	(9.3, 10.4)
$EuCl_3$	5.0 (0.1)	5.0 (0.2)	8.4 (1.0)
	(2.6, 3.4)	(6.1, 7.3)	(7.1, 9.0)
$EuCl_4^-$	3.0 (0.0)	2.7 (0.5)	4.2 (0.6)
	(2.6, 3.4)	(6.2, 7.0)	(5.7, 7.6)
$EuCl_5^{2-}$	2.0 (0.0)	2.0 (0.1)	9.0 (0.4)
	(2.6, 3.4)	(6.1, 7.1)	(7.0, 8.5)
$EuCl_6^{3-}$	9.1 (0.9)	3.3 (0.8)	6.8 (0.6)
	(4.2, 5.9)	(8.3, 8.9)	(6.0, 7.5)

[a] Coordination number and fluctuations (first line) and positions (Å) of the first maximum and minimum (second line). Averages over the last 0.2 ns.

(56) Boumizane, K.; Herzog-Cance, M. H.; Jones, D. J.; Pascal, J. L.; Potier, J.; Roziere, J. *Polyhedron* **1991**, *10*, 2757−2769.
(57) Faithfull, D. L.; Harrowfield, J. M.; Ogden, M. I.; Skelton, B. W.; Third, K.; White, A. H. *Aust. J. Chem.* **1992**, *45*, 583−594.

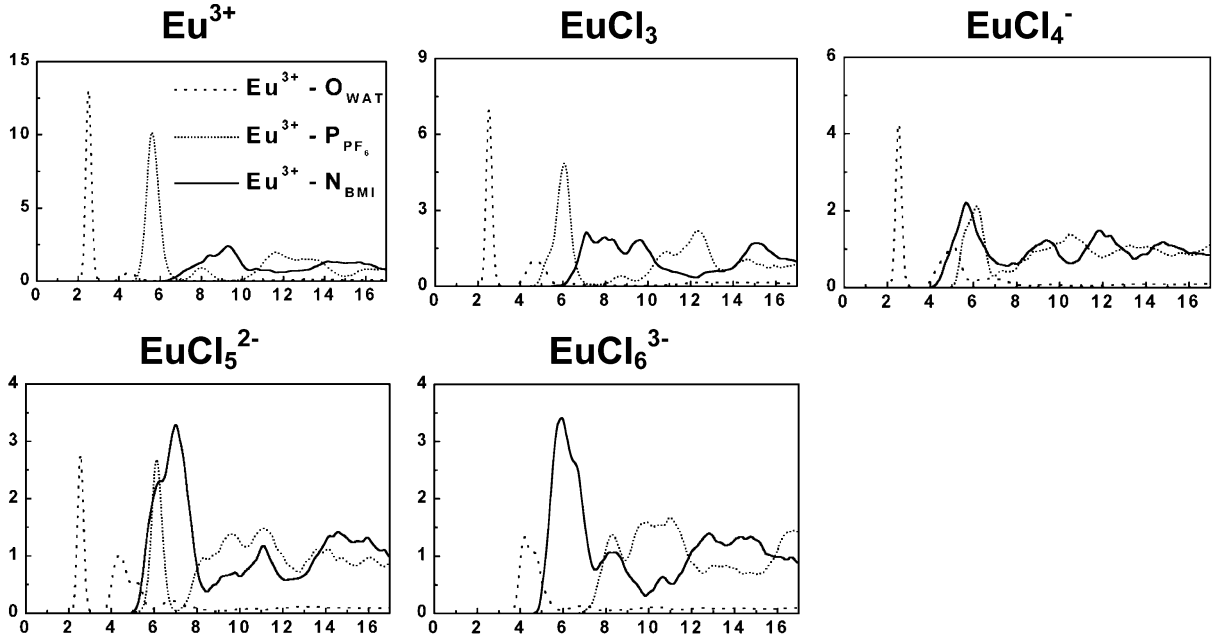

Figure 6. Eu^{3+} and its chloro complexes in the humid IL solution: RDFs of O_{wat}, P_{PF_6}, and N_{BMI} atoms around the Eu atom.

respectively, on the average, within 7.3 Å), stabilized by hydrogen-bonding interactions with the first-shell H_2O ligands on one side and by attractions with the BMI^+ cations on the other side. Within 7.3 Å from the metal, one finds about 9, 13, and 11 "second-shell" H_2O molecules, respectively, around the $EuCl_3$, $EuCl_4^-$, and $EuCl_5^{2-}$ complexes.

Schematically, the saturated $EuCl_6^{3-}$ complex is embedded in a water shell (9.1 H_2O molecules within 5.9 Å), followed by BMI^+ cations (6.8, on the average, within 6.5 Å). About half of the first-shell H_2O molecules display bridging hydrogen bonds over pairs of Cl^- ligands. Interestingly, 9.1 H_2O molecules are not sufficient to solvate the whole complex, and the first shell is completed by BMI^+ cations (about 4, on the average) whose C_2H, C_4H, or C_5H aromatic protons are hydrogen bonded to Cl^- ligands of the complex.

4. Insights into Energy Components of the Uranyl and Europium Solvation in the Humid [BMI][PF_6][H_2O] Liquid. We analyzed the interaction energy ΔE_{solv} between the complexes and the IL, with aims (i) to compare the ΔE_{solv} as a function of the number of Cl^- ligands, (ii) to assess the contributions of the different liquid components, and (iii) to compare the solvation of the humid liquid and the dry liquid (from ref 28). The main results are given in Table 4.

It can be seen that the interaction of the uranyl and europium complexes with the IL is attractive and increases with the number of Cl^- ligands: from −168 kcal/mol (UO_2Cl_2) to −352 ± 15 kcal/mol ($UO_2Cl_4^{2-}$) for the uranyl complexes and from −335 kcal/mol ($EuCl_3$) to −628 ± 20 kcal/mol ($EuCl_6^{3-}$) for the europium complexes. The water contribution to ΔE_{solv} is very important and ranges from 75% to 47% for the uranyl complexes and from 58% to 27% for the europium complexes. It somewhat decreases when metal chlorination increases, which is consistent with stripping of water from the inner sphere of the metal. As expected, the contribution of the PF_6^- anions, small for the neutral UO_2Cl_2 and $EuCl_3$ complexes, becomes increasingly repulsive as the charge of the complex becomes more negative. In all cases, these repulsions are overcompensated by the attractions with the more remote BMI^+ cations. As supported by the structural analyses, this energy analysis points to the role of water in mediating the complex/PF_6^- interactions: the anions are attracted by the H_2O ligands and by the surrounding BMI^+ solvent cations.

It is interesting to compare the change in "solvation energy" ΔE_{solv} with the change in intrinsic (gas-phase) stabilities as a function of the degree of metal chlorination. Indeed, according to quantum mechanical (QM) studies and our force field results, the $EuCl_6^{3-}$ complex is intrinsically unstable and should lose one or two Cl^- ligands to release the "electrostatic strain" in its inner shell.[30,31] The first Cl^- dissociation is exothermic by 107 kcal/mol (DFT B3LYP/6-31+G* calculations) and by 94 kcal/mol (AMBER results). This is much smaller, however, than the loss of solvation energy of $EuCl_5^{2-}$, compared to $EuCl_6^{3-}$ (253 ± 20 kcal/mol), which strongly points to the importance of solvation forces on the stability of $EuCl_6^{3-}$ in the humid IL solution. The same conclusion holds when $EuCl_5^{2-}$ is compared to $EuCl_4^-$, as the former is better solvated (by 100 kcal/mol), and this overcompensates for its intrinsically lower stability (by 32 kcal/mol, according to the QM results).[30,31]

Among the different uranyl complexes, $UO_2Cl_4^{2-}$ is better solvated than $UO_2Cl_3^-$ (by 160 ± 15 kcal/mol), which also largely compensates for its lower intrinsic stability (47 kcal/mol according to the QM studies, and 13 kcal/mol according to the AMBER results; see Figure 8). On the other hand, among the $UO_2Cl_3^-$ and UO_2Cl_2 complexes, the former is stable toward Cl^- dissociation and is better solvated, and should be preferred in the IL solution. Thus, according to this analysis and the MD results, $UO_2Cl_4^{2-}$ is the most stable form of uranyl in the humid liquid.

It is also instructive to compare the solvation of a given cation or complex in the humid versus dry form of the IL.

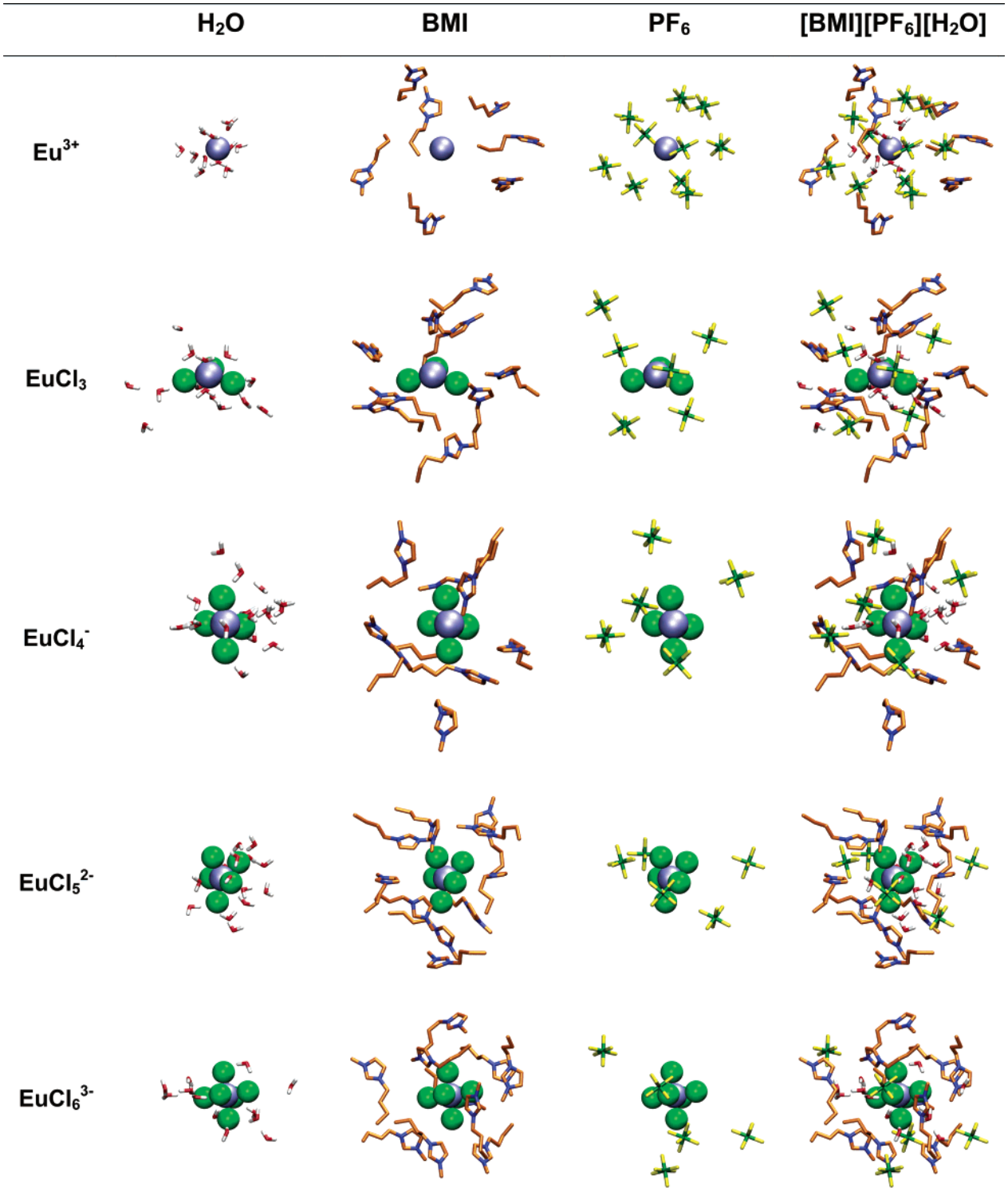

Figure 7. Eu^{3+} and its chloro complexes in the humid IL solution: final snapshots of the first shell (within 9 Å) of U, showing (from left to right) H_2O only, BMI^+ only, PF_6^- only, and the solvent.

Table 4 shows that each species interacts better with the humid than with the dry liquid. The difference is larger for the less halogenated complexes (~70 kcal/mol for UO_2Cl_2 and 180 ± 15 kcal/mol for $EuCl_3$), which take up the largest amount of water, than for the saturated ones (~80 kcal/mol for $UO_2Cl_4^{2-}$ and ~55 ± 15 kcal/mol for $EuCl_6^{3-}$). The naked cations also prefer the humid IL (by ~65 kcal/mol for UO_2^{2+} and 310 kcal/mol for Eu^{3+}).[58] From this analysis, one can conclude that the cations and their chloro complexes are better solvated in the humid ionic liquid and that, among

(58) This may seem somewhat surprising due to the fact that their first shell is anionic in the dry IL, and neutral in the humid IL. In fact, solvation in the humid IL is favored (i) by the metal attraction to inner-shell water molecules, (ii) by its still significant attraction to the somewhat more remote (but less strained) PF_6^- anionic shell, and (iii) by the reduced repulsions from the BMI^+ cations.

Table 4. UO_2^{2+} and Eu^{3+} and Their Chloride Complexes in Humid and Dry IL Solutions: Average Interaction Energies and Fluctuations (kcal/mol) between UO_2^{2+} or Eu^{3+} and the Different Components of Humid IL and Comparison with the Dry IL

	humid IL				dry IL
system	BMI^+	PF_6^-	H_2O	E_{tot}	E_{tot}
UO_2^{2+}	838 (17)	−1084 (18)	−278 (14)	−525 (14)	−461 (13)
UO_2Cl_2	−42 (6)	1 (8)	−127 (10)	−168 (9)	−96 (6)
$UO_2Cl_3^-$	−503 (9)	416 (7)	−105 (10)	−192 (10)	
$UO_2Cl_4^{2-}$	−994 (15)	807 (12)	−165 (17)	−352 (15)	−278 (5)
Eu^{3+}	1222 (21)	−1774 (23)	−615 (13)	−1167 (19)	−856 (16)
$EuCl_3$	−46 (5)	−12 (6)	−277 (12)	−335 (15)	−150 (8)
$EuCl_4^-$	−510 (9)	398 (11)	−165 (13)	−277 (15)	−169 (11)
$EuCl_5^{2-}$	−1067 (15)	838 (12)	−146 (13)	−375 (13)	−298 (12)
$EuCl_6^{3-}$	−1599 (23)	1138 (18)	−168 (16)	−628 (20)	−572 (14)

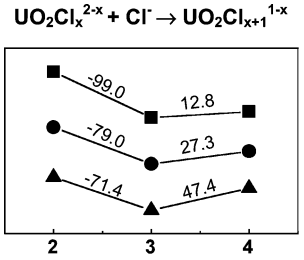

Figure 8. Uranyl complexes in the gas phase: energy changes (kcal/mol) upon complexation of Cl^-, obtained by molecular mechanics (■), HF/6-31+G* (●), and DFT/6-31+G* (▲) calculations with BSSE correction. Total QM energies and structures are given in Table S1.

the different chloro complexes, $UO_2Cl_4^{2-}$ and $EuCl_6^{3-}$ should be most stable in solution.

Discussion and Conclusions

We report a theoretical investigation on the effect of ionic liquid solvent humidity on the solvation of important cations involved in nuclear waste solutions: uranyl and europium, an average-sized lanthanide cation, also a good mimic of trivalent actinides such as Am^{3+} or Cm^{3+}. The results are completely different from those obtained in the dry [BMI]-[PF_6] solutions.[28,29] For instance, in dry conditions, the Eu^{3+} and UO_2^{2+} naked cations coordinate PF_6^- solvent anions in their inner sphere. This contrasts with the humid IL, where they coordinate water only, forming $Eu(H_2O)_9^{3+}$ and $UO_2(H_2O)_5^{2+}$ complexes, solvated by PF_6^- anions in the second shell hydrogen bonded to the H_2O ligands. Similarly, the $EuCl_6^{3-}$ and $UO_2Cl_4^{2-}$ anionic solutes coordinate BMI^+ solvent cations in the dry IL, but prefer water in their first shell in the humid IL, pushing BMI^+ ions somewhat further away. We have seen that hydration is favorable, as far as solute−solvent interactions are concerned. Although the free energies of solvation depend on other factors such as solvent−solvent interactions involving enthalpic and entropic components, the results strongly hint at a larger solubility in the humid than in the dry IL. This conclusion is consistent with spectroscopic results on hydrated versus anhydrous lanthanide salts.[11,59,60]

As concerns the different chloro complexes of a given metal, the calculations show that the saturated $UO_2Cl_4^{2-}$ and $EuCl_6^{3-}$ complexes are intrinsically unstable and should lose at least one Cl^- ligand. In the ionic liquid, however, they are stabilized by solvation forces and should be the most abundant halogenated species, provided that the concentration of Cl^- anions in the solution is sufficient. What happens in humid solution thus depends on the concentration of water and of Cl^- anions. On the computational side, we recently compared two dry "basic" ILs, based on a mixture of Cl^- and $AlCl_4^-$ anions and imidazolium cations, and the amount of saturated complexes that spontaneously formed with UO_2^{2+} and Eu^{3+} during the dynamics was found to increase with the Cl^- concentration.[31] When the hydrated $Eu(H_2O)_8^{3+}$ complex was simulated in these basic melts, H_2O ligands exchanged with the Cl^- anions to form mixed $EuCl_3(H_2O)_4$ and $EuCl_4(H_2O)_3^-$ complexes.[31] This is consistent with recent luminescence spectroscopy results of Eu^{III} in the [BMI][Tf_2N] ionic liquid, as a function of the solvent dryness and of added tetrabutylammonium chloride salt.[11] Because of computer limitations, we did not explore the different water/Cl^- combinations, but the present simulations and those reported in the basic [EMI][TCA] liquid[31] show that "small amounts" of water may dramatically modify the spectroscopic properties of the cations and their complexes. What happens in liquid−liquid extraction conditions (especially when cations are complexed by extractant molecules) also markedly depends on the ionic solvent humidity. The local water content in mixed IL/water systems may even be larger than the one considered in this study (vide infra).

Water Content of the "Humid" Ionic Liquid. Our study was conducted with a 1:1:1 ratio of liquid ions and water, which is more water rich than the pure IL can be, and is more realistic in the presence of highly hydrophilic solutes (e.g., metal cations or their chloro complexes, in equilibrium with uncomplexed Cl^- anions). See also the simulation results of water/IL binary mixtures.[51] Previous work in our group emphasized the importance of interfacial phenomena in classical assisted ion extraction, showing that water and "oil" form a well-defined interface, where presumably the extractant molecules complex the cations.[61−63] It is thus instructive to similarly simulate the aqueous interface with two ILs: [BMI][PF_6] and [OMI][PF_6], where OMI^+ stands for the more hydrophobic 1-octyl-3-methylimidazolium(+) cation (Figure 1). The simulations do not pretend to be quantitative as far as the relative water/IL miscibilities are concerned, but reveal clear effects of the imidazolium substituent on the nature of the interface, and marked differences between these interfaces and those obtained by similar simulations with organic solvents such as chloroform. The final results obtained after 10 ns are shown in Figure 9. The simulations which started with adjacent boxes of neat water and ionic liquid indicate important solvent mixing with the [BMI][PF_6] IL, without formation of a clear-cut interface. The IL phase is very humid, while about 30% of the BMI^+

(59) Branco, L. C.; Rosa, J. N.; Ramos, J. J. M.; Afonso, C. A. M. *Chem.—Eur. J.* **2002**, *8*, 3865−3871.
(60) Lee, S. G.; Park, J. H.; Kang, J.; Lee, J. K. *Chem.—Eur. J.* **2001**, *37*, 785−789.
(61) Wipff, G.; Lauterbach, M. *Supramol. Chem.* **1995**, *6*, 187−207.
(62) Schurhammer, R.; Berny, F.; Wipff, G. *Phys. Chem. Chem. Phys.* **2001**, *3*, 647−656.
(63) Baaden, M.; Burgard, M.; Wipff, G. *J. Phys. Chem. B* **2001**, *105*, 11131−11141.

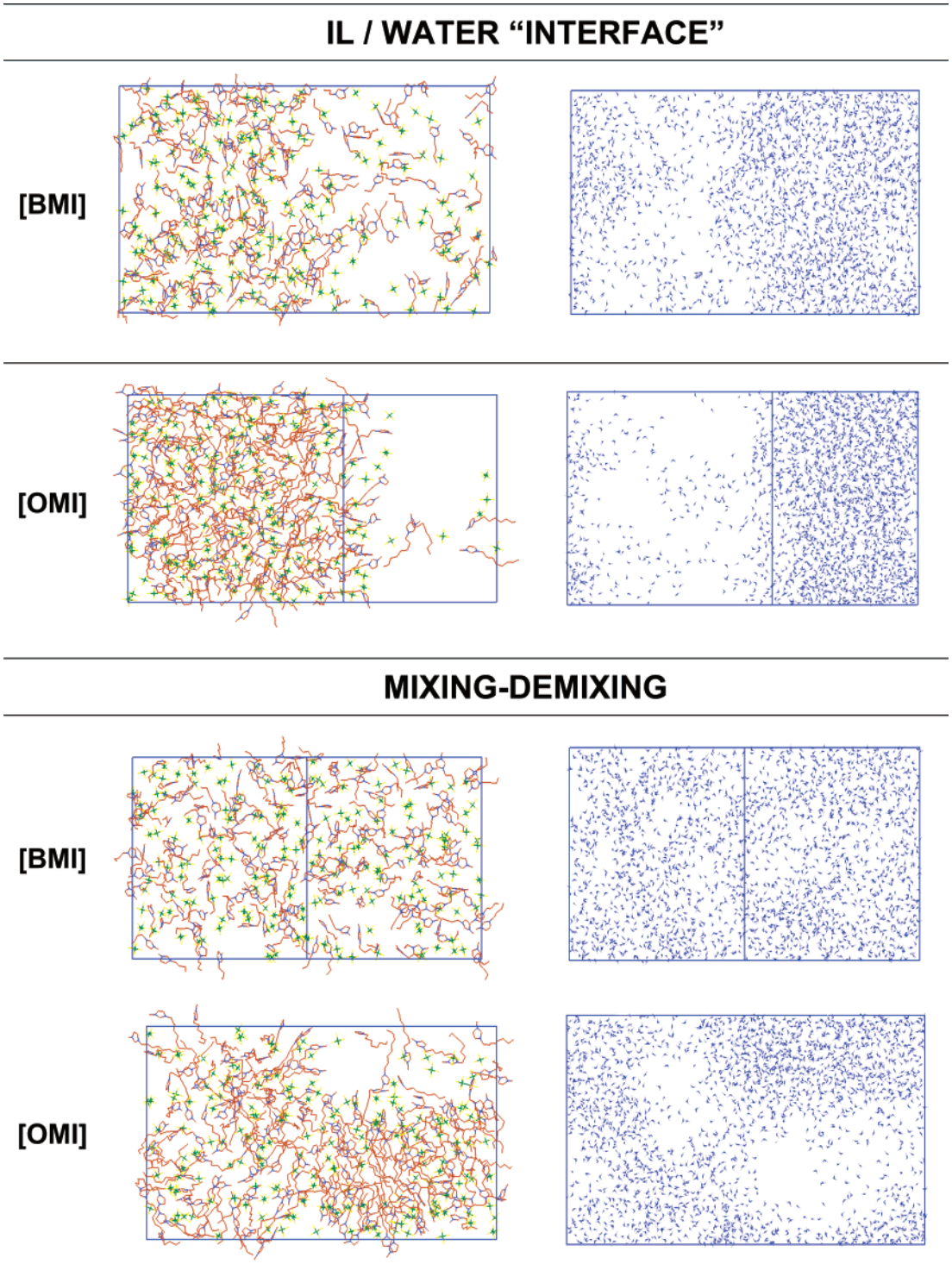

Figure 9. MD simulations on IL/water mixtures: comparison of [BMI][PF_6] vs [OMI][PF_6] liquids. Final snapshots (after 10 ns of dynamics) of simulations which started either from a model-built IL/water interface (IL/water "interface") or from randomly mixed liquids (mixing−demixing) are shown. The IL and water molecules are shown side by side, instead of superimposed, for clarity.

and PF_6^- ions sit "in water", which is much more than the experimental miscibility (1.3×10^{-3} mole fraction of the IL in water).[32] In the same simulation conditions, the more hydrophobic [OMI][PF_6] liquid mixes much less with water, thus leading to a more "abrupt" interface (Figure 9), as observed with classical organic solvents used for liquid−liquid extraction.[62,64] In the latter case, one can clearly distinguish a humid IL phase, adjacent to a water phase containing only a few BMI^+ and PF_6^- ions. Similar differences are observed upon demixing MD simulations with the two ILs, which started with "randomly mixed" phases (Figure 9). Even after 10 ns of demixing simulations, there is no clear phase separation. As a matter of comparison, binary mixtures of water with chloroform[65] or CO_2[66,67] separate

(64) Schweighofer, K. J.; Benjamin, I. *J. Phys. Chem.* **1995**, *99*, 9974−9985.

totally in less than 0.5 ns and form a well-defined interface. The [BMI][PF_6] IL does not separate from water, but forms inhomogeneous domains, some of which are more water rich. With the [OMI][PF_6] ionic liquid, there is some phase separation, without formation of, however, a "flat" interface between slabs of water and IL. One can however clearly recognize water domains containing a few IL ions, and two IL "droplets" of micellar type which are quasi-dry, thus following trends expected from the increased hydrophobicity of the [OMI][PF_6] IL, when compared to [BMI][PF_6]. The extent and outcome of phase separation depend on many factors such as the water/oil ratio, the size and shape of the simulation box, and the nature of solutes,[68] which requires further investigations. The simulated boxes may be too small to depict bulk IL and water phases, next to a broad interfacial region with important solvent mixing. However, these MD experiments point to the importance of water mixing with the IL as a function of its composition. The binary system with the more hydrophobic IL displays marked analogies with water/oil interfaces based on classical organic solvents, or on supercritical CO_2. We believe that these simulation results are important from a mechanistic point of view. They are consistent with the evolution of a cation exchange mechanism with [BMI][PF_6] (upon extraction of the M^{n+} metal, the neutrality of the receiving phase is achieved by releasing BMI^+ cations "to water") to a more classical anion coextraction mechanism with [OMI][PF_6] (M^{n+} drags *n* X^- anions from the aqueous to the ionic liquid phase).[7,27,69−72] The consequences in terms of the nature of the extracted ion and its complexes are presently under investigation in our group.

Note Added in Proof: We recently reran the simulations on aqueous interfaces with [BMI][PF_6] liquids, scaling down the atomic charges of the BMI^+, OMI^+, and PF_6^- ions by a factor 0.9. Such a procedure somewhat mimics the anion-to-cation charge transfer and reduces the IL hydrophilicity. Indeed, after 10 ns of dynamics, there is much less IL/water mixing than shown in Figure 9. Remarkably, at the [BMI][PF_6] interface, the amount of water in the IL (0.28 mol/L) and the amount of IL in water (2×10^{-3} mol/L) nearly match their experimental solubilities.[32] These new calculations confirm the difference between interfaces with BMI^+ versus OMI^+ cations. (Chaumont, A.; Schurhammer, R.; Wipff, G. Presented at RSC Faraday Discussion 129, The Dynamics and Structure of the Liquid−Liquid Interface, Fitzwilliam College, Cambridge, U.K., Sep 1−3, 2004).

Acknowledgment. We are grateful to IDRIS, CINES, the Université Louis Pasteur, and PARIS for computer resources and to E. Engler for his kind assistance.

Supporting Information Available: Figures showing the surface delineated by water in molecules in the humid [BMI][PF_6]-[H_2O] liquid and the hydration number of each of nine UO_2^{2+} and nine Eu^{3+} ions in [BMI][PF_6][H_2O] solution as a function of time and tables giving the total energies, HF- and DFT-optimized structures, and Mulliken charges of the UO_2Cl_2, $UO_2Cl_3^-$, and $UO_2Cl_4^{2-}$ complexes and characteristics of the simulated binary mixtures of IL and water interfaces and mixing/demixing simulations (PDF). This material is available free of charge via the Internet at http://pubs.acs.org.

IC049386V

(65) Muzet, N.; Engler, E.; Wipff, G. *J. Phys. Chem. B* **1998**, *102*, 10772−10788.
(66) Baaden, M.; Schurhammer, R.; Wipff, G. *J. Phys. Chem. B* **2002**, *106*, 434−441.
(67) Schurhammer, R.; Wipff, G. In *Separations and Processes Using Supercritical Carbon Dioxide*; Gopalan, A. S., Wai, C., Jacobs, H., Eds.; American Chemical Society: Washington, DC, 2003; pp 223−244.
(68) Coupez, B.; Boehme, C.; Wipff, G. *J. Phys. Chem. B* **2003**, *107*, 9484−9490.
(69) Visser, A. E.; Swatloski, R. P.; Reichert, W. M.; Griffin, S. T.; Rogers, R. D. *Ind. Eng. Chem. Res.* **2000**, *39*, 3596−3604.
(70) Dietz, M. L.; Dzielawa, J. A. *Chem. Commun.* **2001**, 2124−2125.
(71) Chun, S.; Dzyuba, S. V.; Bartsch, R. A. *Anal. Chem.* **2001**, *73*, 3737−3741.
(72) Dietz, M. L.; Dzielawa, J. A.; Laszak, I.; Young, B. A.; Jensen, M. P. *Green Chem.* **2003**, *5*, 682−685.